Localization of acoustic sources utilizing a decentralized particle filter

Florian Xaver*, Gerald Matz*, Peter Gerstoft‡ and Norbert Goertz*
*Institute of Telecommunications, Vienna University of Technology, Vienna (Austria), florian.xaver@nt.tuwien.ac.at
‡Scripps Institution of Oceanography, University of California, San Diego (CA, USA)

Abstract—**This paper presents recent results of a decentralized localization scheme. Several sensors are embedded in an acoustic wave field. We assume that the field variables of interest are governed by a discrete-time spatial-distributed state-space equation. In particular, acoustic waves are emitted by sources and observed by sensors. For decentralized localization, a further decomposition of the state-space model gives a decentralized model. A decentralized estimation algorithm infers jointly the field and source states. The messages between sensors are sent over an imperfect channel. For qualitative statements of the estimation, its performance is explored by an analytic sequential Weiss-Weinstein bound on the estimation error.**

I. Introduction

In this paper, we address the localization [1, 2] of a source in a spatio-temporal field [3–8]. We assume an acoustic in-door scenario. The acoustic-wave propagation is governed by a discrete-time state-transition equation [3, 9]. Several sensors measure the pressure which is modeled by a measurement equation. To infer the location of an acoustic source, a non-linear source model completes the overall model. The algorithm of a decentralized sequential maximum a-posteriori particle filter (PF) was proposed in [9].

The overall model features three state vectors. The wave propagation is captured by a pressure state vector and a state vector of the time derivative of the pressure states. Both state vectors are spatially distributed and lie on a grid. The third state vector describes the discrete location of the source.

The sequential Weiss-Weinstein bound (SWW) is a sequential Bayesian performance bound which gives a lower bound on the error co-variance of any estimator. A popular bound for Bayesian estimation is the sequential Cramér-Rao (SCR) bound [1, 10, 11]. Our model demands for a bound which jointly supports discrete random location states and continuous field states. Furthermore, the discrete distribution is categorical which means that it has finite support. This leads to the SWW bound [12–15].

Here, we seek for an analytic sequential Bayesian lower bound on the estimation error. As additional novelty, we assume an imperfect channel between the sensors by use of the rate-distortion theory [16, 17]. We address the following main issues:

1) Conditions for existence of analytic SWW solutions.
2) Behavior of the SWW bound on pressure states and sensor location.
3) Sensitivity of the SWW bound to the distortion of the channel.

In Section II, we will present the underlying model. The imperfect channel will be specified in Section III. Next, we will give an analytic SWW bound (Section IV) and numerical results (Section V).

II. Model

In this section, we will summarize the decentralized localization earlier published in [9]. An acoustic source occurs in a hallway. We model the acoustic wave field $\mathbf{\Phi}^{\mathrm{c}}$, the non-linear source ϕ^{cd}, the path of the source $\mathbf{\Phi}^{\mathrm{d}}$, and the measurements $\boldsymbol{C}$. Bold upper-case symbols denote matrices. Above models are governed by following discrete-time state-space model (discrete time k):

$$\begin{bmatrix}\boldsymbol{x}^{\mathrm{c}}_{k+1}\\ \boldsymbol{x}^{\mathrm{d}}_{k+1}\end{bmatrix} = \begin{bmatrix}\mathbf{\Phi}^{\mathrm{c}}\boldsymbol{x}^{\mathrm{c}}_k + \phi^{\mathrm{cd}}(\boldsymbol{x}^{\mathrm{d}}_k)\\ \mathbf{\Phi}^{\mathrm{d}}\boldsymbol{x}^{\mathrm{d}}_k\end{bmatrix} + \begin{bmatrix}\boldsymbol{w}^{\mathrm{c}}_k\\ \boldsymbol{w}^{\mathrm{d}}_k\end{bmatrix} , \tag{1a}$$

$$\boldsymbol{y}_k = \boldsymbol{C}\boldsymbol{x}^{\mathrm{c}}_k + \boldsymbol{v}_k , \tag{1b}$$

with the continuous N-dimensional state vector $\boldsymbol{x}^{\mathrm{c}}_k = [\boldsymbol{q}^{\mathrm{T}}_k, \boldsymbol{p}^{\mathrm{T}}_k]^{\mathrm{T}}$ and the discrete source position vector $\boldsymbol{x}^{\mathrm{d}}_k$. The vector $\boldsymbol{x}^{\mathrm{c}}_k$ captures the pressure on a grid by $\boldsymbol{p}_k$ whereas its time derivative is denoted by $\boldsymbol{q}_k$. Both are distributed over space and $\boldsymbol{p}_k$ represents the sampled wave field. The measurements are denoted by $\boldsymbol{y}_k$. The continuous random vector $\boldsymbol{w}^{\mathrm{c}}_k$ models the process noise of the acoustic wave, vector $\boldsymbol{w}^{\mathrm{d}}_k$ the discrete position jitter, and $\boldsymbol{v}_k$ the continuous measurement noise.

In the decentralized case, $\mathbf{\Phi}^{\mathrm{c}}$ is decomposed into sub-matrices. Every sensor m has an estimator using following sub-state space model:

$$\begin{bmatrix}\boldsymbol{x}^{\mathrm{c},(m)}_{k+1}\\ \boldsymbol{x}^{\mathrm{d},(m)}_{k+1}\end{bmatrix} = \begin{bmatrix}\mathbf{\Phi}^{\mathrm{c},(m)}\boldsymbol{x}^{\mathrm{c},(m)}_k + \bar{\boldsymbol{x}}^{\mathrm{c},(m)}_k + \phi^{\mathrm{cd}}(\boldsymbol{x}^{\mathrm{d},(m)}_k)\\ \mathbf{\Phi}^{\mathrm{d}}\boldsymbol{x}^{\mathrm{d},(m)}_k\end{bmatrix} + \begin{bmatrix}\boldsymbol{w}^{\mathrm{c},(m)}_k\\ \boldsymbol{w}^{\mathrm{d},(m)}_k\end{bmatrix} , \tag{2a}$$

$$\boldsymbol{y}^{(m)}_k = \boldsymbol{C}^{(m)}\boldsymbol{x}^{\mathrm{c},(\mathrm{m})}_k + \boldsymbol{v}^{(m)}_k . \tag{2b}$$

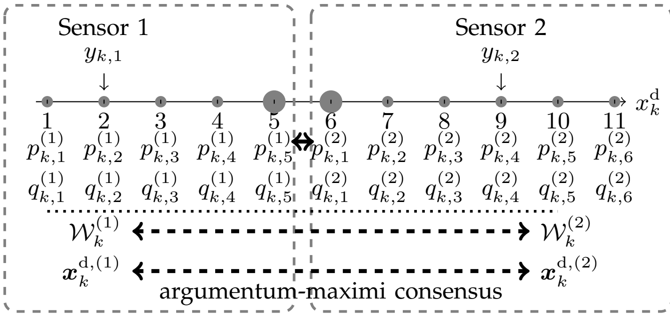

Fig. 1: Decentralized model capturing an 1-D acoustic wave equation. The sample points of the wave model are assigned to two sensors. Arrows denote message exchange. The weights $\mathcal{W}_k^{(m)}$ of the PF and the local belief $\boldsymbol{x}_k^{\mathrm{d},(m)}$ are not exchanged at every time k. The radii of the filled circles denote different noise variance.

Vectors $\boldsymbol{x}_k^{\mathrm{c},(m)}, m = 1, \cdots, M$ are disjoint sub-vectors of $\boldsymbol{x}_k^{\mathrm{c}}$ whereas $\bar{\boldsymbol{x}}_k^{\mathrm{c},(m)}$ is the coupling term between the different sub-state space models (see Figure 1). Similar for vector $\boldsymbol{y}_k^{(m)}$.

Every sensor m has its own copy $\boldsymbol{x}_k^{\mathrm{c},(m)}$ of the global source position vector $\boldsymbol{x}_k^{\mathrm{d}}$. Thus the local MAP estimator of sensor m has a local estimate of the position. A final argumentum-maximi consensus algorithm ensures a joint belief of the position [9]. Observe that the linear sub-structures of (1) and (2) allow the use of the very efficient marginalized particle filter [18].

References [9, 19] assume perfect channels between the sensors, i.e. the coupling term $\bar{\boldsymbol{x}}_k^{\mathrm{c},(m)}$ in (2) is not perturbed. In the sequel we relax this assumption and analyze the impact of imperfect channels.

III. Imperfect channel

Per se, there are no approximation errors inherent in the decentralized model (2) compared to (1). Thus, we use the global model (1) for the following analysis of the estimation error. Additionally, we assume an imperfect channel in the decentralized model which adds distortion to $\bar{\boldsymbol{x}}_k^{\mathrm{c},(m)}$ in (2). This corresponds to additional noise in the centralized model (1), i.e. the imperfect channel perturbs some elements of $\boldsymbol{x}_k^{\mathrm{c}}$.

On that account, we assume that decorrelated signals $\boldsymbol{\iota}_k = \mathrm{decorr}\, \bar{\boldsymbol{x}}_k^{\mathrm{c},(m)}$ are exchanged instead of $\bar{\boldsymbol{x}}_k^{\mathrm{c},(m)}$ [19]. At the sensor's boundary, noise $\sim \mathcal{N}\{0, D\}$ is added to $\boldsymbol{w}_k^{\mathrm{c}}$.

We use following worst-case assumptions:

- Elements of vector $\boldsymbol{\iota}_k$ are Gaussian distributed and are transmitted over an additive Gaussian channel with noise variance $\sigma^2_{\mathrm{channel}}$.
- The channel can be used once per $\boldsymbol{\iota}_k$.
- The average channel input power P_{channel} is limited.

Then the distortion [17]

$$D = \frac{\sigma^2_{\iota_k}}{1 + {P_{\mathrm{channel}}}/{\sigma^2_{\mathrm{channel}}}} \ . \tag{3}$$

IV. Sequential Weiss-Weinstein bound

The hybrid continuous/discrete probability densities and the finite support of the source-position density demand for a more general Bayesian bound than the sequential Cramér-Rao bound: the sequential Weiss-Weinstein bound. Additionally, we must use a general definition of the expectation operator, i.e.

$$\mathrm{E}_{\boldsymbol{x},\boldsymbol{y}}\left\{g(\boldsymbol{x},\boldsymbol{y})\right\} \triangleq \int g(\boldsymbol{x},\boldsymbol{y}) \mathrm{d}P_{\boldsymbol{x},\boldsymbol{y}}(\boldsymbol{x},\boldsymbol{y}) \tag{4}$$

with some measurable function $g(\boldsymbol{x},\boldsymbol{y})$ and the continuous/discrete probability measure $P_{\boldsymbol{x},\boldsymbol{y}}$. We define the N-dimensional vector $\boldsymbol{x}_k \triangleq [\boldsymbol{x}_k^{\mathrm{c},\mathrm{T}}, \boldsymbol{x}_k^{\mathrm{d},\mathrm{T}}]^{\mathrm{T}}$. The sequential WW bound

$$\boldsymbol{W}_k = \boldsymbol{H}_k \boldsymbol{J}_k^{-1} \boldsymbol{H}_k^{\mathrm{T}} \tag{5}$$

of the estimation error $\boldsymbol{\varepsilon}_k = \hat{\boldsymbol{x}}_k(\boldsymbol{y}_k) - \boldsymbol{x}_k$ lower bounds the error co-variance [12, 14]

$$\mathrm{E}\left\{\boldsymbol{\varepsilon_k}\boldsymbol{\varepsilon_k}^{\mathrm{T}}\right\} \succcurlyeq \boldsymbol{W}_k \ . \tag{6}$$

Symbol $\succcurlyeq$ denotes that the right side subtracted from the left gives a positive semi-definite matrix. Matrices $\boldsymbol{W}_k$ correspond to the inverse Fisher information matrices of the sequential Cramér-Rao bound. Matrices $\boldsymbol{H}_k = [\boldsymbol{h}_{k,1}, \cdots, \boldsymbol{h}_{k,N}]$ are parameters of the SWW bound at time k. Optimal matrices $\boldsymbol{H}_k$ give the maximum lower bound of all possible lower bounds of the SWW family.

Matrix $\boldsymbol{J}_k$ is sequentially computed,

$$\boldsymbol{A}_k = \boldsymbol{D}_{k+1}^{11} - \boldsymbol{D}_{k+1}^{10} \boldsymbol{A}_{k-1}^{-1} (\boldsymbol{D}_{k+1}^{10})^{\mathrm{T}} \ , \tag{7a}$$

$$\boldsymbol{J}_{k+1} = \boldsymbol{D}_{k+1}^{22} - \boldsymbol{D}_{k+1}^{21} \boldsymbol{A}_k^{-1} (\boldsymbol{D}_{k+1}^{21})^{\mathrm{T}} \ , \tag{7b}$$

with $\boldsymbol{A}_{-1}^{-1} := \boldsymbol{0}$ and $\boldsymbol{J}_0^{-1}$ is set to the co-variance of the prior. The matrices $\boldsymbol{D}_{k+1}^{ij}$, $i,j \in \{0,1,2\}$ in (7) are defined by

$$[\boldsymbol{D}_{k+1}^{ij}]_{mn} = 2\frac{e^{\mu_1} - e^{\mu_2}}{e^{\mu_3} e^{\mu_4}} \tag{8}$$

with

$$\mu_1 = \mu(\mathfrak{h}_{(k-2+i)N+m}, -\mathfrak{h}_{(k-2+j)N+n}) \ , \tag{9}$$

$$\mu_2 = \mu(\mathfrak{h}_{(k-2+i)N+m}, \mathfrak{h}_{(k-2+j)N+n}) \ , \tag{10}$$

$$\mu_3 = \mu(\mathfrak{h}_{(k-2+i)N+m}, \mathfrak{o}) \ , \tag{11}$$

$$\mu_4 = \mu(\mathfrak{o}, \mathfrak{h}_{(k-2+j)N+n}) \ , \tag{12}$$

where we used

$$[\mathfrak{h}_0, \cdots, \mathfrak{h}_{kN}] := \begin{bmatrix} \boldsymbol{H}_0 & & \\ & \ddots & \\ & & \boldsymbol{H}_k \end{bmatrix} \ . \tag{13}$$

The semi-invariant moment generating function $\mu(\mathfrak{h}_a, \mathfrak{h}_b)$ is given in (14), cf. [12, 14]. Symbol $\mathfrak{o}$ is the zero-vector with the same number of elements as $\mathfrak{h}_0$.

Our aim is to derive the analytic solution of the semi-invariant moment generating function for (1).

$$\mathrm{E}\left\{ \frac{\prod_{\ell=0}^{k+1} \sqrt{v_{\boldsymbol{y}_\ell|\boldsymbol{x}_\ell}(\boldsymbol{y}_\ell|\boldsymbol{x}_\ell + \boldsymbol{h}_{\ell,a}) v_{\boldsymbol{x}_\ell|\boldsymbol{x}_{\ell-1}}(\boldsymbol{x}_\ell + \boldsymbol{h}_{\ell,a}|\boldsymbol{x}_{\ell-1} + \boldsymbol{h}_{\ell-1,a}) v_{\boldsymbol{y}_\ell|\boldsymbol{x}_\ell}(\boldsymbol{y}_\ell|\boldsymbol{x}_\ell - \boldsymbol{h}_{\ell,b}) v_{\boldsymbol{x}_\ell|\boldsymbol{x}_{\ell-1}}(\boldsymbol{x}_\ell - \boldsymbol{h}_{\ell,b}|\boldsymbol{x}_{\ell-1} - \boldsymbol{h}_{\ell-1,b})}}{v_{\boldsymbol{x}_{0:k+1},\boldsymbol{y}_{1:k+1}}(\boldsymbol{x}_{0:k+1}, \boldsymbol{y}_{1:k+1})} \right\} \tag{14}$$

Theorem 1 (SWW of non-linear transition model)**.** *Given the non-linear state-space model* (1) *where* $\boldsymbol{x}_k^{\mathrm{c}} \sim f(\boldsymbol{x}_0^{\mathrm{c}})$, $\boldsymbol{x}_0^{\mathrm{d}} \sim p(\boldsymbol{x}_k^{\mathrm{d}})$, $\boldsymbol{w}_k^{\mathrm{c}} \sim f(\boldsymbol{w}_k^{\mathrm{c}})$, $\boldsymbol{w}_k^{\mathrm{d}} \sim p(\boldsymbol{w}_k^{\mathrm{d}})$ *and* $\boldsymbol{v}_k \sim f(\boldsymbol{v}_k)$*. Function* f *denotes a continuous,* p *a discrete and* v *a hybrid discrete/continuous density.*

Then the semi-invariant moment generating function μ *is given in* (18) *and* (19) *in the Appendix using the definition*

$$\xi_{\boldsymbol{x}}(\boldsymbol{h}) \triangleq e^{-\frac{1}{8}\|\boldsymbol{h}\|^2_{\boldsymbol{C}_{\boldsymbol{x}}}} \tag{15}$$

and the initial conditions

$$v(\boldsymbol{y}_0|\boldsymbol{x}_0)v(\boldsymbol{x}_0|\boldsymbol{x}_{-1}) := v(\boldsymbol{y}_0)v(\boldsymbol{x}_0) \ . \tag{16}$$

The proof is in the Appendix. We get an analytic result if the sums in (18) and (19) are finite. They are finite if and only if the transition probability mass function has finite support.

Corollary 2 (Categorical distribution)**.** *Given a mixed continuous/discrete state space model with a non-linearity as in* (1)*. If the probability density of the discrete random states is categorical, then an analytic sequential SWW bound exists.*

Tab. I: Simulation settings (cf. Figure 1)

Densities	
$f(\boldsymbol{q}_0) \sim \mathcal{N}\{0, 0.0001\boldsymbol{I}\}$	$p(x_0^{\mathrm{d}}) \sim \mathcal{U}\{4, 8\}$
$f(\boldsymbol{p}_0) \sim \mathcal{N}\{0, 0.01\boldsymbol{I}\}$	$f(\boldsymbol{w}_k^{\mathrm{c,p}}) \sim \mathcal{N}\{0, 0.01\boldsymbol{I}\}$
$f(\boldsymbol{w}_k^{\mathrm{c,q}}) \sim \mathcal{N}\{0, 0.25\boldsymbol{I}\}$	$f(\boldsymbol{v}_k) \sim \mathcal{N}\{0, 0.01\boldsymbol{I}\}$
Symmetric triangular density as transition density	
$p(x_k^{\mathrm{d}}\|x_{k-1}^{\mathrm{d}}) = \begin{cases} 0.9\ , & x_k^{\mathrm{d}} = x_{k-1}^{\mathrm{d}} \\ 0.05\ , & x_k^{\mathrm{d}} = x_{k-1}^{\mathrm{d}} \pm 1\ , \\ 0.95\ , & x_k^{\mathrm{d}} = x_{k-1}^{\mathrm{d}} \in \{1, 11\}\ , \\ 0.1\ , & x_k^{\mathrm{d}} = 10,\ x_{k-1}^{\mathrm{d}} = 11\ , \\ 0.1\ , & x_k^{\mathrm{d}} = 2,\ x_{k-1}^{\mathrm{d}} = 1\ , \\ 0\ , & \text{else} \end{cases}$	
State-space model	
ϕ^{cd}: source function, $\boldsymbol{\Phi}^{\mathrm{c}}$: discretized 1-D field, $\boldsymbol{\Phi}^{\mathrm{d}} = 1$	
$\phi^{\mathrm{cd}} : x_k^{\mathrm{d}} \mapsto 0.68\boldsymbol{e}_{6+x_k^{\mathrm{d}}}$	$\boldsymbol{C}$ picks pressure state at $2\,\&\,9$
$[\boldsymbol{\Phi}^{\mathrm{c}}]_{1,1} = 0.98$	$[\boldsymbol{\Phi}^{\mathrm{c}}]_{i,i} = 1, i \in [2, 22]$
$[\boldsymbol{\Phi}^{\mathrm{c}}]_{i+11,i} = 5.8 \times 10^{-5}, i \in [1, 11]$	
$[\boldsymbol{\Phi}^{\mathrm{c}}]_{i,i+11} = -3.4, i \in [1, 11]$	
$[\boldsymbol{\Phi}^{\mathrm{c}}]_{i,i+12} = 1.7, i \in [2, 10]$	$[\boldsymbol{\Phi}^{\mathrm{c}}]_{1,13} = 3.4$
$[\boldsymbol{\Phi}^{\mathrm{c}}]_{i+1,i+11} = 1.7, i \in [1, 10]$	
Parameters of the SWW for $k = 1, 2, \cdots$	
$\boldsymbol{H}_0 = \boldsymbol{H}_k = \text{blockdiag}\left(0.01Q\left(\boldsymbol{\Phi}^{\mathrm{cT}}\right), 1\right)$	

V. Numerical Results

The SWW bound (5) of state-space model (1) with additional noise (3) from an imperfect channel is analyzed in the following.

Figure 1 shows the setup for our analysis: Two sensors are in an one-dimensional grid of 11 nodes. The grid is partitioned into two similar sub-grids associated with the nearest sensors. On the left side, we assume a transparent boundary. On the right side, a wall is modeled. One source occurs at time $k = 1$. The settings are summarized in Table I. Function $Q(\boldsymbol{A})$ replaces every non-zero element in $\boldsymbol{A}$ by 1 and $\boldsymbol{e}_\ell$ is a zero vector except the ℓ^{th} entry which is one.

Figure 2a shows the bound on the pressure states for one instant of time. It features low values at sensor positions and an error floor in-between. At the boundary between sensors, additional noise from the channel's distortion has a low influence on the neighborhood. Observe that the bound depends linearly on the additional distortion. The noise diffuses over several time steps.

The bound on the $\boldsymbol{q}$-states is plotted in Figure 2b. Observe that the bound depends non-linearly on the additional distortion.

The bound on the localization-error variance is plotted in Figure 2c. According to (18) and (19), the parameters $\boldsymbol{H}_k$ at time k also influence the computation at time $k \pm 1$. The minimum at time $k = 2$ is caused by different support of prior and transition density whereas $\boldsymbol{H}_0 = \boldsymbol{H}_1$.

VI. Conclusions

Hybrid continuous/categorical distributions of prior and noise demand for a more general sequential Bayesian bound than the SCR bound: the SWW bound. Although a non-linearity is inherent in the state space model, there exist analytic solutions of the SWW bound. At a specific time step, the SWW bound of the pressure states stays approximately constant over location. The SWW bound of the source location is insensitive to noise introduced by the imperfect channel between sensors.

Appendix

Proof of Theorem 1: Due to (13), many $\boldsymbol{h}$ vectors in (14) are zero and thus we omit them. For any time ℓ, the pairs of densities with $\boldsymbol{h}_{\ell,a} = \boldsymbol{h}_{\ell,b} = \boldsymbol{0}$ and $\boldsymbol{h}_{\ell-1,a} = \boldsymbol{h}_{\ell-1,b} = \boldsymbol{0}$ are separable from the rest. They cancel.

If either $\boldsymbol{h}_{\ell,a}$, $\boldsymbol{h}_{\ell,b}$, $\boldsymbol{h}_{\ell-1,a}$, or $\boldsymbol{h}_{\ell-1,b}$ has elements unequal zero, the product

$$\begin{aligned} &v(\boldsymbol{x}_\ell + \boldsymbol{h}_{\ell,a}|\boldsymbol{x}_{\ell-1} + \boldsymbol{h}_{\ell-1,a})v(\boldsymbol{x}_\ell - \boldsymbol{h}_{\ell,b}|\boldsymbol{x}_{\ell-1} - \boldsymbol{h}_{\ell-1,b}) \\ &= f(\boldsymbol{x}_\ell^{\mathrm{c}} + \boldsymbol{h}_{\ell,a}|\boldsymbol{x}_{\ell-1}^{\mathrm{c}} + \boldsymbol{h}_{\ell-1,a}^{\mathrm{c}}, \boldsymbol{x}_{\ell-1}^{\mathrm{d}} + \boldsymbol{h}_{\ell+1,a}^{\mathrm{d}}) \\ &\times f(\boldsymbol{x}_\ell^{\mathrm{c}} - \boldsymbol{h}_{\ell,b}|\boldsymbol{x}_{\ell-1}^{\mathrm{c}} - \boldsymbol{h}_{\ell-1,b}^{\mathrm{c}}, \boldsymbol{x}_{\ell-1}^{\mathrm{d}} - \boldsymbol{h}_{\ell-1,b}^{\mathrm{d}}) \\ &\times p(\boldsymbol{x}_\ell^{\mathrm{d}} + \boldsymbol{h}_{\ell,a}^{\mathrm{d}}|\boldsymbol{x}_{\ell-1}^{\mathrm{d}} + \boldsymbol{h}_{\ell-1,a}^{\mathrm{d}})p(\boldsymbol{x}_\ell^{\mathrm{d}} - \boldsymbol{h}_{\ell,b}^{\mathrm{d}}|\boldsymbol{x}_{\ell-1}^{\mathrm{d}} - \boldsymbol{h}_{\ell-1,b}^{\mathrm{d}})\ . \end{aligned} \tag{17}$$

Inserting the definitions of the Gaussian distribution and the discrete uniform distribution gives the result (cf. the proofs in [12]).

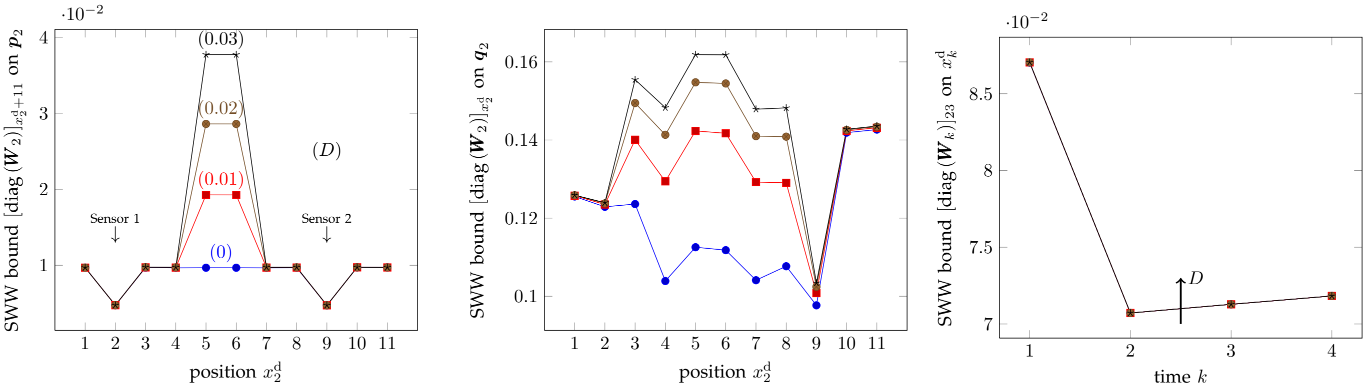

(a) (b) (c)

Fig. 2: Sequential Weiss-Weinstein bound on the error variance of (a) pressure states $\boldsymbol{p}_2$, (b) $\boldsymbol{q}_2$ states, and (c) the x_k^{d} state. Due to an imperfect channel, states $q_{2,5}$ and $q_{2,6}$ are added by Gaussian noise $\mathcal{U}\{0, D\}$.
Legend: $D = 0$ (—●—), $D = 0.01$ (—■—), $D = 0.02$ (—●—), $D = 0.03$ (—⋆—)

References

[1] B. Ristic, S. Arulampalam, and N. Gordon, *Beyond the Kalman Filter: Particle Filters for Tracking Applications*. Boston: Artech House, 2004.

[2] O. Hlinka, O. Slučiak, F. Hlawatsch, P. Djurić and, and M. Rupp, "Likelihood consensus and its application to distributed particle filtering," *IEEE Transactions on Signal Processing*, vol. 60, no. 8, pp. 4334–4349, Aug. 2012. DOI: 10.1109/TSP.2012.2196697.

[3] F. Xaver, C. F. Mecklenbräuker, P. Gerstoft, and G. Matz, "Distributed state and field estimation using a particle filter," in *Proc. 44th Asilomar Conference on Signals, Systems, and Computers*, Pacific Grove, CA, Nov. 2010, pp. 1447–1451. DOI: 10.1109/ACSSC.2010.5757775.

[4] F. Sawo, "Nonlinear state and parameter estimation of spatially distributed systems," PhD thesis, Universität Karlsruhe, 2009.

[5] T. van Waterschoot and G. Leus, "Distributed estimation of static fields in wireless sensor networks using the finite element method," in *IEEE International Conference on Acoustics, Speech and Signal Processing (ICASSP)*, Mar. 2012, pp. 2853–2856. DOI: 10.1109/ICASSP.2012.6288512.

[6] I. Dokmanic and M. Vetterli, "Room helps: acoustic localization with finite elements," in *IEEE International Conference on Acoustics, Speech and Signal Processing (ICASSP)*, Mar. 2012, pp. 2617–2620. DOI: 10.1109/ICASSP.2012.6288453.

[7] H. Yao, P. Gerstoft, P. M. Shearer, and C. F. Mecklenbräuker, "Compressive sensing of the Tohoku-Oki mw 9.0 earthquake: Frequency-dependent rupture modes," *Geophysical Research Letters*, vol. 38, no. L20310, pp. 1–5, 2011. DOI: 10.1029/2011GL049223.

[8] F. Jensen, W. Kuperman, M. Porter, and H. Schmidt, *Computational Ocean Acoustics*, 1st ed. New York: American Institute of Physics Press, 1994.

[9] F. Xaver, G. Matz, P. Gerstoft, and C. F. Mecklenbräuker, "Localization of acoustic sources using a decentralized particle filter," *EURASIP Journal on Wireless Communications and Networking*, vol. 2011, no. 1, p. 94, 2011. DOI: 10.1186/1687-1499-2011-94.

[10] P. Tichavsky, C. Muravchik, and A. Nehorai, "Posterior Cramer-Rao bounds for discrete-time nonlinear filtering," *IEEE Transactions on Signal Processing*, vol. 46, no. 5, pp. 1386–1396, 1998. DOI: 10.1109/78.668800.

[11] H. Van Trees and K. Bell, *Bayesian bounds for parameter estimation and nonlinear filtering/tracking*. IEEE Press, 2007.

[12] F. Xaver, G. Matz, P. Gerstoft, and C. F. Mecklenbräuker, "Analytic sequential Weiss-Weinstein bounds," unpublished.

[13] I. Rapoport and Y. Oshman, "Recursive weiss-weinstein lower bounds for discrete-time nonlinear filtering," in *43rd IEEE Conference on Decision and Control*, vol. 3, Dec. 2004, pp. 2662–2667. DOI: 10.1109/CDC.2004.1428862.

[14] ——, "Weiss-Weinstein lower bounds for markovian systems. Part 1: Theory," *Signal Processing, IEEE Transactions on*, vol. 55, no. 5, pp. 2016–2030, May 2007. DOI: 10.1109/TSP.2007.893208.

[15] A. Renaux, P. Forster, P. Larzabal, C. Richmond, and A. Nehorai, "A fresh look at the Bayesian bounds of the Weiss-Weinstein family," *IEEE Transactions on Signal Processing*, vol. 56, no. 11, pp. 5334–5352, 2008.

[16] T. Cover and J. Thomas, *Elements of information theory*. Wiley-Interscience, 2006.

[17] N. Goertz, *Joint source-channel coding of discrete-time signals with continuous amplitudes*. Imperial College Press, 2007.

[18] T. Schon, F. Gustafsson, and P. Nordlund, "Marginalized particle filters for mixed linear/nonlinear state-space models," *IEEE Transactions on Signal Processing*, vol. 53, no. 7, pp. 2279–2289, 2005.

[19] F. Xaver, G. Matz, P. Gerstoft, and C. F. Mecklenbräuker, "Predictive state vector encoding for decentralized field estimation in sensor networks," in *IEEE International Conference on Acoustics, Speech and Signal Processing (ICASSP)*, Mar. 2012, pp. 2661–2664. DOI: 10.1109/ICASSP.2012.6288464.

$$
\begin{aligned}
D_1^{11}:\mu(\mathfrak{h}_a,\mathfrak{h}_b) =& \ln \sum_{\boldsymbol{x}_1^{\mathrm{d}}} \sum_{\boldsymbol{x}_0^{\mathrm{d}}} \xi_{\boldsymbol{w}_0^{\mathrm{c}}} \left(-\boldsymbol{\Phi}^{\mathrm{c}} \boldsymbol{h}_{0,a}^{\mathrm{c}} - \boldsymbol{\Phi}^{\mathrm{c}} \boldsymbol{h}_{0,b}^{\mathrm{c}} - \Phi^{\mathrm{cd}}(\boldsymbol{x}_0^{\mathrm{d}} + \boldsymbol{h}_{0,a}^{\mathrm{d}}) + \Phi^{\mathrm{cd}}(\boldsymbol{x}_0^{\mathrm{d}} - \boldsymbol{h}_{0,b}^{\mathrm{d}}) \right) \xi_{\boldsymbol{x}_0^{\mathrm{c}}}(\boldsymbol{h}_{0,a}^{\mathrm{c}} + \boldsymbol{h}_{0,b}^{\mathrm{c}}) \\
& \times p(\boldsymbol{x}_1^{\mathrm{d}} | \boldsymbol{x}_0^{\mathrm{d}} + \boldsymbol{h}_{0,a}^{\mathrm{d}})^{1/2} p(\boldsymbol{x}_1^{\mathrm{d}} | \boldsymbol{x}_0^{\mathrm{d}} - \boldsymbol{h}_{0,b}^{\mathrm{d}})^{1/2} p(\boldsymbol{x}_0^{\mathrm{d}} + \boldsymbol{h}_{0,a}^{\mathrm{d}})^{1/2} p(\boldsymbol{x}_0^{\mathrm{d}} - \boldsymbol{h}_{0,b}^{\mathrm{d}})^{1/2} \qquad (18a)\\
D_2^{11}:\mu(\mathfrak{h}_a,\mathfrak{h}_b) =& \ln \xi_{\boldsymbol{v}_1^{\mathrm{c}}}(\boldsymbol{C}\boldsymbol{h}_{1,a} + \boldsymbol{C}\boldsymbol{h}_{1,b}) \\
& \times \sum_{\boldsymbol{x}_2^{\mathrm{d}}} \cdots \sum_{\boldsymbol{x}_0^{\mathrm{d}}} \xi_{\boldsymbol{w}_1^{\mathrm{c}}} \left(-\boldsymbol{\Phi}^{\mathrm{c}} \boldsymbol{h}_{1,a}^{\mathrm{c}} - \boldsymbol{\Phi}^{\mathrm{c}} \boldsymbol{h}_{1,b}^{\mathrm{c}} - \Phi^{\mathrm{cd}}(\boldsymbol{x}_1^{\mathrm{d}} + \boldsymbol{h}_{1,a}^{\mathrm{d}}) + \Phi^{\mathrm{cd}}(\boldsymbol{x}_1^{\mathrm{d}} - \boldsymbol{h}_{1,b}^{\mathrm{d}}) \right) \xi_{\boldsymbol{w}_0^{\mathrm{c}}}(\boldsymbol{h}_{1,a}^{\mathrm{c}} + \boldsymbol{h}_{1,b}^{\mathrm{c}}) \\
& \times p(\boldsymbol{x}_2^{\mathrm{d}} | \boldsymbol{x}_1^{\mathrm{d}} + \boldsymbol{h}_{1,a}^{\mathrm{d}})^{1/2} p(\boldsymbol{x}_2^{\mathrm{d}} | \boldsymbol{x}_1^{\mathrm{d}} - \boldsymbol{h}_{1,b}^{\mathrm{d}})^{1/2} \times p(\boldsymbol{x}_1^{\mathrm{d}} + \boldsymbol{h}_{1,a}^{\mathrm{d}} | \boldsymbol{x}_0^{\mathrm{d}})^{1/2} p(\boldsymbol{x}_1^{\mathrm{d}} - \boldsymbol{h}_{1,b}^{\mathrm{d}} | \boldsymbol{x}_0^{\mathrm{d}})^{1/2} p(\boldsymbol{x}_0^{\mathrm{d}}) \qquad (18b)\\
D_{k+1}^{11}:\mu(\mathfrak{h}_a,\mathfrak{h}_b) =& \ln \xi_{\boldsymbol{v}_k^{\mathrm{c}}}(\boldsymbol{C}\boldsymbol{h}_{k,a} + \boldsymbol{C}\boldsymbol{h}_{k,b}) \\
& \times \sum_{\boldsymbol{x}_{k+1}^{\mathrm{d}}} \cdots \sum_{\boldsymbol{x}_0^{\mathrm{d}}} \xi_{\boldsymbol{w}_k^{\mathrm{c}}} \left(-\boldsymbol{\Phi}^{\mathrm{c}} \boldsymbol{h}_{k,a}^{\mathrm{c}} - \boldsymbol{\Phi}^{\mathrm{c}} \boldsymbol{h}_{k,b}^{\mathrm{c}} - \Phi^{\mathrm{cd}}(\boldsymbol{x}_k^{\mathrm{d}} + \boldsymbol{h}_{k,a}^{\mathrm{d}}) + \Phi^{\mathrm{cd}}(\boldsymbol{x}_k^{\mathrm{d}} - \boldsymbol{h}_{k,b}^{\mathrm{d}}) \right) \xi_{\boldsymbol{w}_{k-1}^{\mathrm{c}}}(\boldsymbol{h}_{k,a}^{\mathrm{c}} + \boldsymbol{h}_{k,b}^{\mathrm{c}}) \\
& \times p(\boldsymbol{x}_{k+1}^{\mathrm{d}} | \boldsymbol{x}_k^{\mathrm{d}} + \boldsymbol{h}_{k,a}^{\mathrm{d}})^{1/2} p(\boldsymbol{x}_{k+1}^{\mathrm{d}} | \boldsymbol{x}_k^{\mathrm{d}} - \boldsymbol{h}_{k,b}^{\mathrm{d}})^{1/2} \times p(\boldsymbol{x}_k^{\mathrm{d}} + \boldsymbol{h}_{k,a}^{\mathrm{d}} | \boldsymbol{x}_{k-1}^{\mathrm{d}})^{1/2} p(\boldsymbol{x}_k^{\mathrm{d}} - \boldsymbol{h}_{k,a}^{\mathrm{d}} | \boldsymbol{x}_{k-1}^{\mathrm{d}})^{1/2} \\
& \times \prod_{\ell=0}^{k-2} p(\boldsymbol{x}_{\ell+1}^{\mathrm{d}} | \boldsymbol{x}_\ell^{\mathrm{d}}) f_{\boldsymbol{x}_0^{\mathrm{d}}}(\boldsymbol{x}_0^{\mathrm{d}}) \qquad (18c)\\
D_1^{22}:\mu(\mathfrak{h}_a,\mathfrak{h}_b) =& \ln \xi_{\boldsymbol{v}_1^{\mathrm{c}}}(\boldsymbol{C}\boldsymbol{h}_{1,a} + \boldsymbol{C}\boldsymbol{h}_{1,b}) \sum_{\boldsymbol{x}_1^{\mathrm{d}}} \sum_{\boldsymbol{x}_0^{\mathrm{d}}} \xi_{\boldsymbol{w}_0^{\mathrm{c}}}(\boldsymbol{h}_{1,a}^{\mathrm{c}} + \boldsymbol{h}_{1,b}^{\mathrm{c}}) \times p(\boldsymbol{x}_1^{\mathrm{d}} + \boldsymbol{h}_{1,a}^{\mathrm{d}} | \boldsymbol{x}_0^{\mathrm{d}})^{1/2} p(\boldsymbol{x}_1^{\mathrm{d}} - \boldsymbol{h}_{1,a}^{\mathrm{d}} | \boldsymbol{x}_0^{\mathrm{d}})^{1/2} p(\boldsymbol{x}_0^{\mathrm{d}}) \qquad (18d)\\
D_{k+1}^{22}:\mu(\mathfrak{h}_a,\mathfrak{h}_b) =& \ln \xi_{\boldsymbol{v}_{k+1}^{\mathrm{c}}}(\boldsymbol{C}\boldsymbol{h}_{k+1,a} + \boldsymbol{C}\boldsymbol{h}_{k+1,b}) \sum_{\boldsymbol{x}_{k+1}^{\mathrm{d}}} \cdots \sum_{\boldsymbol{x}_0^{\mathrm{d}}} \xi_{\boldsymbol{w}_k^{\mathrm{c}}}(\boldsymbol{h}_{2,a}^{\mathrm{c}} + \boldsymbol{h}_{2,b}^{\mathrm{c}}) \\
& \times p(\boldsymbol{x}_{k+1}^{\mathrm{d}} + \boldsymbol{h}_{k+1,a}^{\mathrm{d}} | \boldsymbol{x}_k^{\mathrm{d}})^{1/2} p(\boldsymbol{x}_{k+1}^{\mathrm{d}} - \boldsymbol{h}_{k+1,a}^{\mathrm{d}} | \boldsymbol{x}_k^{\mathrm{d}})^{1/2} \times \prod_{\ell=0}^{k-1} p(\boldsymbol{x}_{\ell+1}^{\mathrm{d}} | \boldsymbol{x}_\ell^{\mathrm{d}}) p(\boldsymbol{x}_0^{\mathrm{d}}) \qquad (18e)
\end{aligned}
$$

$$
\begin{aligned}
D_2^{10}:\mu(\mathfrak{h}_a,\mathfrak{h}_b) =& \ln \xi_{\boldsymbol{v}_{k+1}^{\mathrm{c}}}(-\boldsymbol{C}\boldsymbol{h}_{1,a}) \sum_{\boldsymbol{x}_2^{\mathrm{d}}} \cdots \sum_{\boldsymbol{x}_0^{\mathrm{d}}} \xi_{\boldsymbol{w}_1^{\mathrm{c}}}(-\boldsymbol{\Phi}^{\mathrm{c}} \boldsymbol{h}_{2,a}^{\mathrm{c}} - \Phi^{\mathrm{cd}}(\boldsymbol{x}_1^{\mathrm{d}} + \boldsymbol{h}_{1,a}^{\mathrm{d}}) + \Phi^{\mathrm{cd}}(\boldsymbol{x}_1^{\mathrm{d}})) \\
& \times \xi_{\boldsymbol{w}_0^{\mathrm{c}}}(\boldsymbol{h}_{1,a}^{\mathrm{c}} - \Phi^{\mathrm{cd}}(\boldsymbol{x}_0^{\mathrm{d}}) - \boldsymbol{\Phi}^{\mathrm{c}} \boldsymbol{h}_{0,b}^{\mathrm{c}} + \Phi^{\mathrm{cd}}(\boldsymbol{x}_0^{\mathrm{d}}) - \boldsymbol{h}_{0,b}^{\mathrm{c}}) \xi_{\boldsymbol{x}_0^{\mathrm{c}}}(\boldsymbol{h}_{0,b}^{\mathrm{c}}) \times p(\boldsymbol{x}_2^{\mathrm{d}} | \boldsymbol{x}_1^{\mathrm{d}} + \boldsymbol{h}_{1,a}^{\mathrm{d}})^{1/2} p(\boldsymbol{x}_2^{\mathrm{d}} | \boldsymbol{x}_1^{\mathrm{d}})^{1/2} \\
& \times p(\boldsymbol{x}_1^{\mathrm{d}} + \boldsymbol{h}_{1,a}^{\mathrm{d}} | \Phi^{\mathrm{d}}(\boldsymbol{x}_0^{\mathrm{d}}))^{1/2} p(\boldsymbol{x}_1^{\mathrm{d}} | \boldsymbol{x}_0^{\mathrm{d}} - \boldsymbol{h}_{0,b}^{\mathrm{d}})^{1/2} p(\boldsymbol{x}_0^{\mathrm{d}})^{1/2} p(\boldsymbol{x}_0^{\mathrm{d}} - \boldsymbol{h}_{0,b}^{\mathrm{d}})^{1/2} \qquad (19a)\\
D_{k+1}^{10}:\mu(\mathfrak{h}_a,\mathfrak{h}_b) =& \ln \xi_{\boldsymbol{v}_{k+1}^{\mathrm{c}}}(-\boldsymbol{C}\boldsymbol{h}_{k+1,a}) \xi_{\boldsymbol{v}_k^{\mathrm{c}}}(\boldsymbol{C}\boldsymbol{h}_{k,b}) \\
& \times \sum_{\boldsymbol{x}_{k+1}^{\mathrm{d}}} \cdots \sum_{\boldsymbol{x}_0^{\mathrm{d}}} \xi_{\boldsymbol{w}_k^{\mathrm{c}}}(-\boldsymbol{\Phi}^{\mathrm{c}} \boldsymbol{h}_{k,a}^{\mathrm{c}} - \Phi^{\mathrm{cd}}(\boldsymbol{x}_k^{\mathrm{d}} + \boldsymbol{h}_{k,a}^{\mathrm{d}}) + \Phi^{\mathrm{cd}}(\boldsymbol{x}_k^{\mathrm{d}})) \\
& \times \xi_{\boldsymbol{w}_{k-1}^{\mathrm{c}}}(\boldsymbol{h}_{k,a}^{\mathrm{c}} - \Phi^{\mathrm{cd}}(\boldsymbol{x}_{k-1}^{\mathrm{d}}) - \boldsymbol{\Phi}^{\mathrm{c}} \boldsymbol{h}_{k-1,b}^{\mathrm{c}} + \Phi^{\mathrm{cd}}(\boldsymbol{x}_{k-1}^{\mathrm{d}}) - \boldsymbol{\Phi}^{\mathrm{c}} \boldsymbol{h}_{k-1,b}^{\mathrm{c}}) \xi_{\boldsymbol{w}_{k-2}^{\mathrm{c}}}(\boldsymbol{h}_{k-1,b}^{\mathrm{c}}) \\
& \times p(\boldsymbol{x}_{k+1}^{\mathrm{d}} | \boldsymbol{x}_k^{\mathrm{d}} + \boldsymbol{h}_{k,a}^{\mathrm{d}})^{1/2} p(\boldsymbol{x}_{k+1}^{\mathrm{d}} | \boldsymbol{x}_k^{\mathrm{d}})^{1/2} \times p(\boldsymbol{x}_k^{\mathrm{d}} + \boldsymbol{h}_{k,a}^{\mathrm{d}} | \boldsymbol{x}_{k-1}^{\mathrm{d}})^{1/2} p(\boldsymbol{x}_k^{\mathrm{d}} | \boldsymbol{x}_{k-1}^{\mathrm{d}} - \boldsymbol{h}_{k-1,b}^{\mathrm{d}})^{1/2} \\
& \times \prod_{\ell=0}^{k-2} p(\boldsymbol{x}_{\ell+1}^{\mathrm{d}} | \boldsymbol{x}_\ell^{\mathrm{d}}) p(\boldsymbol{x}_0^{\mathrm{d}}) \qquad (19b)\\
D_1^{12}:\mu(\mathfrak{h}_a,\mathfrak{h}_b) =& \ln \xi_{\boldsymbol{v}_1^{\mathrm{c}}}(\boldsymbol{C}\boldsymbol{h}_{1,b}) \\
& \times \sum_{\boldsymbol{x}_1^{\mathrm{d}}} \sum_{\boldsymbol{x}_0^{\mathrm{d}}} \xi_{\boldsymbol{w}_1^{\mathrm{c}}}(-\boldsymbol{\Phi}^{\mathrm{c}} \boldsymbol{h}_{0,a}^{\mathrm{c}} - \Phi^{\mathrm{cd}}(\boldsymbol{x}_0^{\mathrm{d}} + \boldsymbol{h}_{0,a}^{\mathrm{d}}) + \boldsymbol{h}_{1,b}^{\mathrm{c}} + \Phi^{\mathrm{cd}}(\boldsymbol{x}_0^{\mathrm{d}})) \xi_{\boldsymbol{x}_0^{\mathrm{c}}}(\boldsymbol{h}_{0,a}^{\mathrm{c}}) \\
& \times p(\boldsymbol{x}_1^{\mathrm{d}} | \boldsymbol{x}_0^{\mathrm{d}} + \boldsymbol{h}_{0,a}^{\mathrm{d}})^{1/2} p(\boldsymbol{x}_1^{\mathrm{d}} - \boldsymbol{h}_{1,b}^{\mathrm{d}} | \boldsymbol{x}_0^{\mathrm{d}})^{1/2} p(\boldsymbol{x}_0^{\mathrm{d}} + \boldsymbol{h}_{0,a}^{\mathrm{d}})^{1/2} p(\boldsymbol{x}_0^{\mathrm{d}})^{1/2} \qquad (19c)\\
D_{k+1}^{12}:\mu(\mathfrak{h}_a,\mathfrak{h}_b) =& \ln \xi_{\boldsymbol{v}_k^{\mathrm{c}}}(\boldsymbol{C}\boldsymbol{h}_{k,a}) \xi_{\boldsymbol{v}_{k+1}^{\mathrm{c}}}(\boldsymbol{C}\boldsymbol{h}_{k+1,b}) \\
& \times \sum_{\boldsymbol{x}_{k+1}^{\mathrm{d}}} \cdots \sum_{\boldsymbol{x}_0^{\mathrm{d}}} \xi_{\boldsymbol{w}_k^{\mathrm{c}}}(-\boldsymbol{\Phi}^{\mathrm{c}} \boldsymbol{h}_{k,a}^{\mathrm{c}} - \Phi^{\mathrm{cd}}(\boldsymbol{x}_k^{\mathrm{d}} + \boldsymbol{h}_{k,a}^{\mathrm{d}}) + \boldsymbol{h}_{k+1,b}^{\mathrm{c}} + \Phi^{\mathrm{cd}}(\boldsymbol{x}_k^{\mathrm{d}})) \xi_{\boldsymbol{x}_{k-1}^{\mathrm{c}}}(\boldsymbol{h}_{k,a}^{\mathrm{c}}) \\
& \times p(\boldsymbol{x}_{k+1}^{\mathrm{d}} | \boldsymbol{x}_k^{\mathrm{d}} + \boldsymbol{h}_{k,a}^{\mathrm{d}})^{1/2} p(\boldsymbol{x}_{k+1}^{\mathrm{d}} - \boldsymbol{h}_{k+1,b}^{\mathrm{d}} | \boldsymbol{x}_k^{\mathrm{d}})^{1/2} \times p(\boldsymbol{x}_k^{\mathrm{d}} + \boldsymbol{h}_{k,a}^{\mathrm{d}} | \boldsymbol{x}_{k-1}^{\mathrm{d}})^{1/2} p(\boldsymbol{x}_k^{\mathrm{d}} | \boldsymbol{x}_{k-1}^{\mathrm{d}})^{1/2} \\
& \times \prod_{\ell=0}^{k-1} p(\boldsymbol{x}_{\ell+1}^{\mathrm{d}} | \boldsymbol{x}_\ell^{\mathrm{d}}) p(\boldsymbol{x}_0^{\mathrm{d}}) \qquad (19d)
\end{aligned}
$$